

## 40% tunneling magnetoresistance after anneal at 380 °C for tunnel junctions with iron–oxide interface layers

Zongzhi Zhang<sup>a)</sup>

*Instituto de Engenharia de Sistemas e Computadores (INESC), R. Alves Redol 9, 1000 Lisbon, Portugal*

S. Cardoso and P. P. Freitas

*Instituto de Engenharia de Sistemas e Computadores (INESC), R. Alves Redol 9, 1000 Lisbon and Departamento de Física, Instituto Superior Técnico (IST), Avenue Rovisco Pais, 1096 Lisbon, Portugal*

X. Batlle

*Departamento Física Fundamental, Universitat Barcelona, Avenue Diagonal 647, 08028 Barcelona, Catalonia, Spain*

P. Wei, N. Barradas, and J. C. Soares

*Instituto Tecnológico e Nuclear, E.N.10 Sacavem and Centro de Física Nuclear da Universidade de Lisboa, Campo Grande, Portugal*

Spin tunnel junctions fabricated with one interposed Fe–FeOx layer between the Al<sub>2</sub>O<sub>3</sub> barrier and the top CoFe pinned electrode show large tunneling magnetoresistance (TMR) (40%) for anneals up to 380 °C. The annealing temperature  $T_{\text{TMR}}^*$ , where maximum TMR occurs, increases with the inserted Fe–FeOx layer thickness. For samples with thicker inserted layer, the pinned layer moment (which usually starts to decay below 300 °C in the normal junctions) increases with annealing temperature up to 380 °C and remains at a maximum until 450 °C. The large TMR at high temperature is related with the diffusion of extra Fe (from the Fe–FeOx layer) into the electrode interfacial region and the as-deposited paramagnetic FeOx decomposition into metallic Fe, and possibly the formation of some Fe<sub>3</sub>O<sub>4</sub>, which compensate the interface polarization loss associated with Mn interdiffusion. Rutherford backscattering spectrometry analysis confirms partial Fe diffusion into the top CoFe electrode after anneal. Meanwhile, x-ray photoelectron spectra for the Fe 2*p* core level show that the FeOx contribution in the upper part of the inserted layer decreases upon annealing, while it increases in the inner part near the barrier, suggesting the FeOx decomposition and the oxygen diffusion toward the inner metallic Fe and Al barrier. The study of  $R \times A$  values and barrier parameters versus annealing temperature for samples with 7 and 25 Å Fe–FeOx also reflects the above structural changes in the inserted layer. © 2001 American Institute of Physics. [DOI: 10.1063/1.1356712]

Magnetic tunnel junctions (MTJs) with tunneling magnetoresistance signal (TMR) in excess of 40% and adjustable resistance-area products  $R \times A$  from 10<sup>6</sup> to few hundred  $\Omega \mu\text{m}^2$  can now be fabricated. The present TMR signals and  $R \times A$  values are suitable for magnetic random access memory applications. However, good thermal stability for the MTJs is required to cope with standard backend processes [sintering: 400–450 °C, plasma enhanced chemical vapor deposition oxide deposition: 350 °C] occurring during MTJ integration with a (CMOS) wafer.<sup>1,2</sup> The TMR signal usually decreases above 300 °C due to the polarization loss resulting from the Mn (in Mn–*X* exchange layer) diffusion into the CoFe top electrode.<sup>3,4</sup> In this work, thermal stability for MTJs is improved up to 380 °C by the insertion of an iron–oxide layer with appropriate thickness between the AlOx barrier and the top CoFe pinned electrode. This brings MTJs one step closer to full CMOS backend compatibility.<sup>5,6</sup>

Junctions with structure of glass/Ta90 Å/Ni<sub>80</sub>Fe<sub>20</sub>70 Å/Co<sub>80</sub>Fe<sub>20</sub>30 Å/Al9 Å+oxide/Fe ( $t_{\text{Fe}}$ ) + oxide/Co<sub>80</sub>Fe<sub>20</sub>40 Å/Mn<sub>76</sub>Fe<sub>24</sub>250 Å/Ti<sub>10</sub>W<sub>90</sub>(N)150 Å were pre-

pared by ion beam deposition and oxidation using a Nordiko 3000 IBD tool, and then patterned down to  $3 \times 1 \mu\text{m}^2$  dimensions with a self-aligned process.<sup>7,8</sup> Magnetic measurements were done by a vibrating sample magnetometer in unpatterned parts of the sample. X-ray photoelectron spectroscopy (XPS) experiments were performed to analyze the Fe and FeOx spatial distribution. Since the XPS signal comes from an area within a distance of about  $2\lambda$ – $3\lambda$  ( $\lambda$  is the inelastic mean free path for electrons) from the sample surface, low-energy ion beam (4 keV, 45°) etch was carried out to obtain a depth profile. Steps 1 and 2 correspond to surface spectra, and step 6 is the spectrum taken after sputtering for 6 s so that step *n* is taken after sputtering for  $6 \cdot (n - 2)$  s. The etch rate is around 6–10 nm/min. The intensities of the photoelectron lines were recorded using the Al *K*<sub>α</sub> emission line. All thermal treatments consist of 45 min anneals at each temperature, done in vacuum (10<sup>−6</sup> Torr), and followed by cooling in field applied along the common easy axis of the electrodes.

Figure 1 shows the pinned layer moments versus annealing temperature for samples with  $t_{\text{Fe}} = 0, 7, 10, 20,$  and 25 Å. The Fe and Al layers are oxidized by 10 s exposure to a remote oxygen plasma except for the Al barrier in the refer-

<sup>a)</sup> Author to whom correspondence should be addressed; electronic mail: zongzhi.zhang@inesc.pt

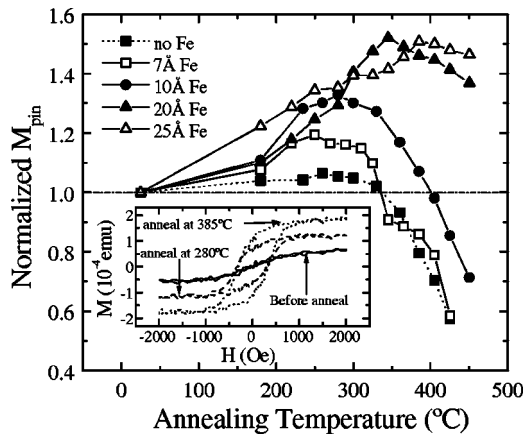


FIG. 1. Dependence of the normalized pinned layer moments on the annealing temperature for various inserted Fe layer thicknesses. The inset shows hysteresis loops for a multilayer with structure of  $(\text{Fe}20 \text{ \AA}/10 \text{ s oxide})_8$  before and after anneal.

ence sample with  $t_{\text{Fe}}=0$ , which is oxidized for 20 s. There is a net increase in the moment of the pinned layer for increasing Fe thickness. For junctions with 7 and 10 Å Fe, there is a strong moment decrease starting around 300 °C, similar to the reference sample without Fe, corresponding to Mn diffusion into the CoFe top electrode. For 25 Å Fe, the pinned layer moment increases almost linearly with annealing temperature up to 380 °C, and remains at a maximum value up to 450 °C. RBS experiments on a special sample of  $\text{Si}/\text{Al}_2\text{O}_3 \text{ 500 \AA}/\text{Co}_{80}\text{Fe}_{20}30\text{ \AA}/\text{Al}9 \text{ \AA}+10 \text{ s oxide}/\text{Fe}20 \text{ \AA}+10 \text{ s oxide}/\text{Co}_{80}\text{Fe}_{20}40 \text{ \AA}/\text{Al}_2\text{O}_3 \text{ 15 \AA}$  shows that  $16.5 \times 10^{+15}$  atom/cm<sup>2</sup> of Fe are found in the as-deposited Fe–FeOx. After anneal at 385 °C,  $7 \times 10^{+15}$  atom/cm<sup>2</sup> of Fe have moved into the top CoFe electrode (about 8 Å increase in the top CoFe thickness, and an enrichment in Fe of the interfacial CoFe region). The remaining  $9.5 \times 10^{+15}$  atom/cm<sup>2</sup> of Fe either form a pure 11 Å thick Fe layer at the AlOx/CoFe interface, with the excess oxygen becoming incorporated into the AlOx barrier, or remaining as FeOx ( $\text{Fe}_3\text{O}_4$ ). To check the magnetic nature of the FeOx grown in this experiment, a multilayer of glass  $/[\text{Fe}20 \text{ \AA}/10 \text{ s oxide}]_8$  was made and was subject to the same annealing procedure described before. The inset shows the as-deposited  $M-H$  loop (characteristic from a paramagnetic FeOx) and loops annealed at 280 and 385 °C (remanence and large coercivity suggest the formation of a ferromagnetic or ferrimagnetic oxide layer, possibly  $\text{Fe}_3\text{O}_4$ ). This proves the nonmagnetic characteristic of the as-deposited FeOx layers. From the above analyses, the moment increase upon anneal comes from the as-deposited nonmagnetic or paramagnetic FeOx decomposition into pure Fe and/or  $\text{Fe}_3\text{O}_4$ , and partial Fe diffusion into the CoFe electrode. It is found that the moment decrease normally due to Mn interdiffusion has been pushed to high temperature for the samples with a thicker Fe–FeOx layer.

Figure 2(a) shows the TMR versus annealing temperature for the samples discussed above. There are striking differences in the as-deposited TMR and annealing temperature  $T_{\text{TMR}}^*$  where maximum TMR occurs, as shown in the inset for various Fe–FeOx thicknesses. In the as-deposited state,

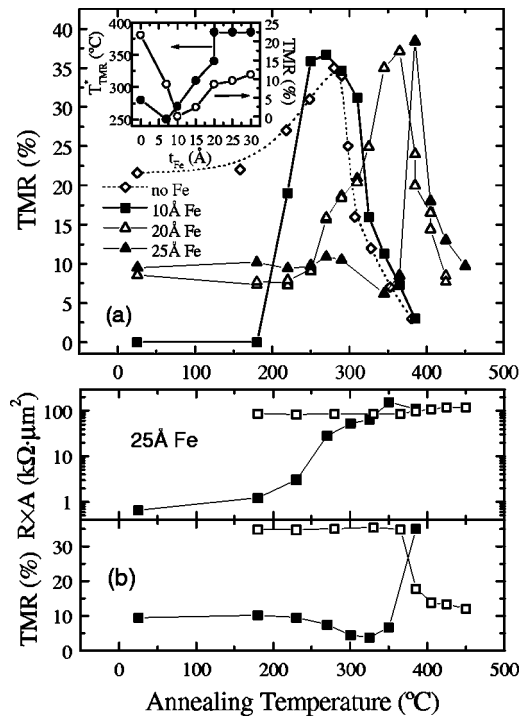


FIG. 2. (a) TMR vs annealing temperature for junctions with different interfacial Fe–FeOx layers. The inset shows the dependence of the as-deposited TMR value and  $T_{\text{TMR}}^*$  (where maximum TMR value occurs) on the inserted layer thickness. (b) TMR and  $R \times A$  values for junctions with 25 Å Fe, first annealed to get the maximum signal (solid square) at 380 °C, then subject to further annealing starting at 180 °C (open square).

full oxidation occurs for  $t_{\text{Fe}}=10 \text{ \AA}$ , and zero TMR results, consistent with formation of a nonmagnetic or paramagnetic Fe oxide. The 8% signal for 7 Å Fe is probably due to a discontinuous Fe layer. For thicker Fe layers, the as-deposited TMR signal is 10%, implying that incomplete oxidation occurs ( $\text{FeOx}+\text{Fe}$  formed).  $T_{\text{TMR}}^*$  increases with the inserted Fe layer thickness, and reaches a maximum of 380 °C at  $t_{\text{Fe}}=20 \text{ \AA}$ . Upon annealing, the TMR signal starts to increase from 0% at 220 °C to 36% at 270 °C in the sample with 10 Å Fe, indicating that the FeOx decomposition starts at 220 °C. For the thicker Fe layers ( $t_{\text{Fe}} \geq 20 \text{ \AA}$ ), TMR first decreases to zero as the annealing temperature increases to 360 °C, and then shows a sharp peak at 380 °C. The TMR decrease is related with the reduced interfacial polarization, occurring when the oxygen from the FeOx layer moves toward the inner metallic Fe, resulting in the paramagnetic FeOx formation near the barrier. The sharp peak at 380 °C is probably associated with the final decomposition of this interfacial FeOx. Figure 2(b) illustrates the stability of such junctions with  $t_{\text{Fe}}=25 \text{ \AA}$  upon reanneal. The sample was first annealed up to 380 °C and showed maximum TMR (solid square). It was then reannealed up to 365 °C (open square) maintaining the large TMR.

In order to clarify what is happening after anneal to the as-deposited Fe–FeOx layer, XPS measurements were performed on a special sample with a structure of  $\text{Si}/\text{Al}_2\text{O}_3 \text{ 1000 \AA}/\text{Co}_{80}\text{Fe}_{20}30 \text{ \AA}/\text{Al}9 \text{ \AA}+10 \text{ s oxide}/\text{Fe}20 \text{ \AA}+10 \text{ s oxide}/\text{Co}_{80}\text{Fe}_{20}40 \text{ \AA}/\text{Ta}30 \text{ \AA}$ . Normalized XPS spectra for the Fe 2p core level ( $2p_{3/2}$  and  $2p_{1/2}$ ) are displayed in

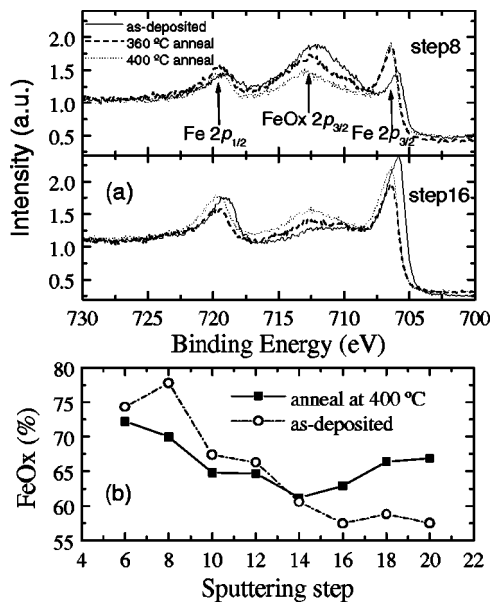


FIG. 3. (a) Normalized intensity of the XPS spectra for the Fe 2p core level (2p<sub>3/2</sub> and 2p<sub>1/2</sub>) showing the metallic Fe and FeOx contributions near the FeOx/CoFe interface (step 8) and near the AlOx/Fe–FeOx interface (step 16) after different anneals. (b) Relative intensity of FeOx as a function of sputtering step for samples in the as-deposited state and annealed at 400 °C.

Fig. 3(a), showing the metallic Fe and FeOx contributions, after different anneals. The two spectra shown here correspond to two different regions of the Fe–FeOx layer: the upper part near the top CoFe interface (step 8, 36 s sputtering), and the inner part near the barrier (step 16, 84 s sputtering), respectively. Figure 3(b) shows the relative intensity of the FeOx contribution in the as-deposited state and annealed at 400 °C, as a function of sputtering time. Near the CoFe interface (step 8), the FeOx contribution decreases upon anneal, revealing the decomposition of the FeOx layer and oxygen moving into the inner Fe layer. Near the AlOx interface (step 16), the relative intensity of the FeOx peak increases with annealing due to the oxygen coming from the decomposition of the initial (outer) FeOx layer, while the intensity of the metal peak decreases.

Figure 4 shows  $R \times A$  values and barrier parameters for two samples with  $t_{Fe} = 7$  and 25 Å. The current–voltage curves were fitted using the Simmons model. The as-deposited  $R \times A$  value for 7 Å Fe is about 9.6 MΩ μm<sup>2</sup> due to full oxidation of the Fe layer, 4 orders larger than that in the sample with 25 Å Fe which is only about 600 Ω μm<sup>2</sup>, but after anneal, both samples reach a similar value. In the as-deposited state, the sample with 7 Å Fe has an effective thickness of about 20 Å and barrier height of 0.5 eV. After anneal at 250 °C where the maximum TMR occurs, the barrier height increases up to 2.5 eV and barrier effective thickness decreases to 10 Å. For 25 Å Fe the as-deposited barrier parameters and the  $R \times A$  value are characteristic of pure 9 Å barrier junctions. Upon annealing, the barrier height de-

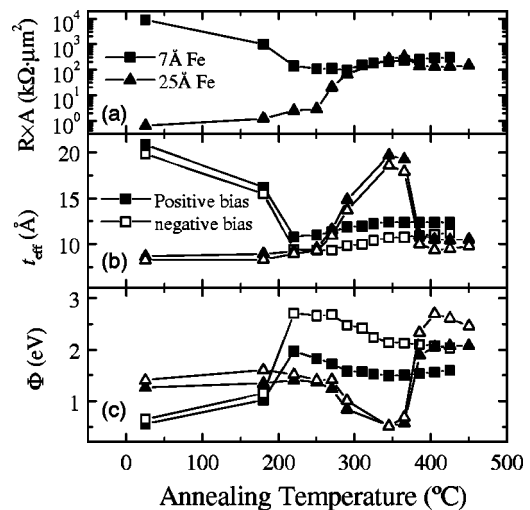


FIG. 4. Resistance–area products, effective barrier height, and barrier thickness for junctions with inserted Fe layers of 7 and 25 Å.

creases to 0.5 eV, but barrier thickness doubles to 20 Å at 360 °C, the barrier parameters at this temperature are similar to the sample of 7 Å Fe in the as-deposited state, indicating the possible same Fe and FeOx distribution existing in these two states. This can be caused by the oxygen migration from the FeOx toward the inner pure Fe near the barrier. Resistance drops at 380 °C where maximum TMR occurs, and at this point barrier height increases from 0.5 to 2.5 eV, and barrier thickness decreases to 10 Å due to the eventual FeOx decomposition at the Al<sub>2</sub>O<sub>3</sub>/Fe interface, in agreement with the XPS results.<sup>9</sup>

This work was supported by PRAXIS XXI Project No. P/CTM/10220/98 and Sapiens Project No. 34116/99. Z.Z. and S.C. are grateful for the support of post-doctoral Grant No. PRAXIS/BPD/22112/99 and PhD Grant No. PRAXIS/BD/11533/97, respectively. X.B. is indebted to Dr. J. Alay (University of Barcelona) for the XPS measurements. Financial support from both the Spanish CICYT through Project No. MAT97-0404 and the Catalanian CIRIT through Project No. 1998SGR0048 are greatly appreciated.

- <sup>1</sup>R. Scheurlein, W. Gallagher, S. S. Parkin, A. Lee, S. Ray, R. Robertazzi, and W. Reohr, Proceedings of the 2000 IEEE International Solid-State Circuits Conference, San Francisco, Feb. 2000, paper TA 7.2.
- <sup>2</sup>S. Tehrani, J. M. Slaughter, E. Chen, M. Durlam, J. Shi, and M. De Herrera, IEEE Trans. Magn. **35**, 2814 (1999).
- <sup>3</sup>S. Cardoso, P. P. Freitas, C. de Jesus, P. Wei, and J. C. Soares, Appl. Phys. Lett. **76**, 610 (2000).
- <sup>4</sup>S. Cardoso, R. Ferreira, P. P. Freitas, P. Wei, and J. C. Soares, Appl. Phys. Lett. **76**, 3792 (2000).
- <sup>5</sup>M. Sharma, C. Fery, S. X. Wang, T. C. Anthony, and J. H. Nickel, IEEE Trans. Magn. (in press).
- <sup>6</sup>R. Jansen and J. S. Moodera, Appl. Phys. Lett. **75**, 400 (1999).
- <sup>7</sup>S. Cardoso, V. Gehanno, R. Ferreira, and P. P. Freitas, IEEE Trans. Magn. **35**, 2952 (1999).
- <sup>8</sup>Z. Zhang, S. Cardoso, P. Wei, N. Barradas, J. C. Soares, and P. P. Freitas, Appl. Phys. Lett. (submitted).
- <sup>9</sup>T. S. Chin and N. C. Chiang, J. Appl. Phys. **81**, 5250 (1997).